86 KSME Journal, Vol.4, No.1, pp. 86~91, 1990.

DISPLACEMENT MEASUREMETS AROUND CRACK TIPS BY DIGITAL AND CONVENTIONAL LASER SPECKLE

M.A. Hamed*

(*Received Junuary 27, 1989*)

The use of optical experimental methods in fracture mechanics has become of great importance since they are easily applied and give a more accurate result than conventional experimental methods. As one of these methods, Laser Speckle Photography was used to determine the displacement field around the crack-tip in a tensile C-specimen. An analytical data analysis was applied including an investigation of rigid body motion. The results were compared with the Westergaard solution and a discussion about this comparison is given. The application of digital image processing and digital data Analysis to the crack-tip problem is also discussed.

Key Words: Crack Tip, Speckle Photography, Laser Speckle, Fringe Analysis

1. INTRODUCTION

In the last decade numerous optical methods have been added to the above mentioned techniques. A major distinction of most of these techniques is the use of coherent light. This group can further be divided into two closely related categories: Holographic Interferometry and Speckle -Metrology. Holographic Interferometry was initially demonstrated by Ennos(1968) who measured in-plane surface strains. Laser Speckle Metrology involves the most recent optical techniques applied to fracture mechanice. Two major categories of speckle metrology exist: Speckle Photography and Speckle Interferomentry. Stetson(1970) defines that Speckle Photography in general involves illumination of an object with a single diverging laser beam and photographing the response before and after the object is moved. He defines Speckle Interferometry methods as those which have an optical setup that corresponds to some type of inteferometer, that is, there are two beams illuminating the object and these beams optically interfere. Still the response must be recorded before and after deformation of the object.

An experiment using the specklegram technique was carried out by Evans and Luxmoore(1974). They measured the in -plane displacements around a crack-tip in a single edge crack tensile specimen made of Araldite CT 200. Their results were compared with the Westergaard solution and showed reasonable agreement. The conclusion did point out though that a major drawback for this technique is the fact that, along with the deformation, rigid body motion effects are also recorded and high precision in the measurements are required to minimize these effects in the recorded data.

Leendertz(1970) measured in-plane displacements of a surface by illuminating it with two laser beams from the same laser symmetrically positioned around the surface normal. The resultant of the two speckle-patterns is recorded before and after movement on the same photographic film. By measuring correlation between the resultant pattern at two different times. a change of relative phase is detected, which in turn gives a measure of surface displacements.

For each of the optical methods mentioned above it has been implied that an optical analysis of a specklegram is necessary. To avoid both the specklegram and the optical analysis a method utilizing digital image processing of speckle-patterns as well as a digital fringe-analysis has been presented by Ranson, Fraley and Hamed(1981).

The objective of this work is to measure the in-plane displacements around a crack tip using a PMMA C-specimen with the purpose that results later on can be applied to cylindrical shaped designs directly.

2. FRINGE FORMATION AND ANALYSIS

2.1 Conventional Analysis

The theory of Young's fringes, states that when two light sources, displaced by a distanced, emittes light with the same wavelength, then the interference of the waves will be both in -phase and out of phase called respectively constructive and destructive interference. Viewed on a screen this interference will appear as bright bands(called fringes)separated by dark bands.

When a diffuse surface is illuminated with coherent light,e. g. a laser beam, the microscopic irregularities of the surface will produce a random interference pattern, effectively acting as a random arrangement of fixed point light sources. When viewed by a lens, adjacent points will, in general, not be resolved and the image will consist of bright and dark areas having a size which are related to the resolving power of the lens. The image of the surface therefore appears as a grainy or "speckled" pattern which can be photographed on a high resolution emulsion. Consider now two identical speckle patterns, displaced by a small distance d in the same plane.

*Depariment of Mechanical Eegineering King Abdulaziz University Jeddah, Saudi Arabia

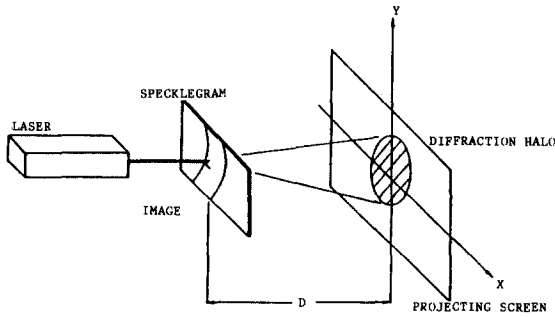

Fig. 1 Pointwise data analysis

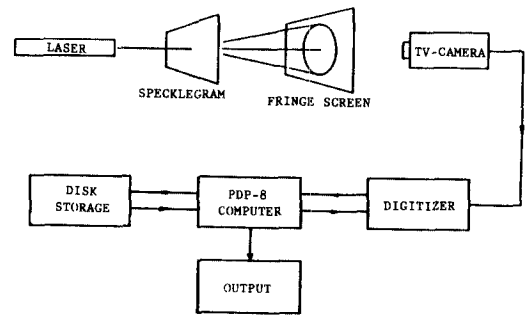

Fig. 2 Schematic of devises used for fringe analysis

Coherent light illuminating each pair of identical speckles will be scattered, and the overlap produces in interference pattern directly analogous to the classical Young's experiment. The diffraction halo showing the fringes was illustrated in Fig. 1. The fringe spacing f which is the distance between the centers of two dark bands in inversly proportional to the displacement d and they are related by the following equation:

$$f=\lambda D/d \tag{1}$$

where D is the distance from the scattering speckles to the screen and the wavelength. The above description is in essence a method to determine the displacement field of a deformed object. The two identical speckle-patterns are originated in the same surface, one recorded before and one after the deformation on the same photographic negative. The result is a double exposure photograph called a specklegram. Obtaining the diffraction halo by illuminating any point of interest and using Eq.(1) we get the displacement of the corresponding surface point. This method is simply called the point-by-point method. If the fringe angle α is also measured then the displacements in the x-and y-direction, u and v, are given by:

$$u=d\cos\alpha$$
$$v=d\sin\alpha \tag{2}$$

where d is the total displacement obtained by Eq.(1).

2.2 Digital Fringe Analysis

It is possible to avoid the inaccuracies of the conventionally measured fringe spacings and angles by using fringe analysis. Schematically the procedure is illustrated in Fig. 2. The diffraction halo is obtained on a translucent screen on which the TV-camera is focused so that it views an image similar to Fig. 1 The TV-picture is composed of 256 lines of video with 240 pixels per line of video. In digitizing the image, each pixel is assigned an integer proportional to the light intensity. Then 10 lines are averaged using a fifteenth order Fourier Transform by means of a Fortran program. The final result is a smoothed curve from which the spacing is calculated. Fig. 3a and Fig. 3b are plots of two data-points separated by 0.12 inches in the specklegram obtained for a C-specimen. The spacing is calculated as numbers of pixels. Knowing the magnification of the TV-lens plus the length of one pixel a

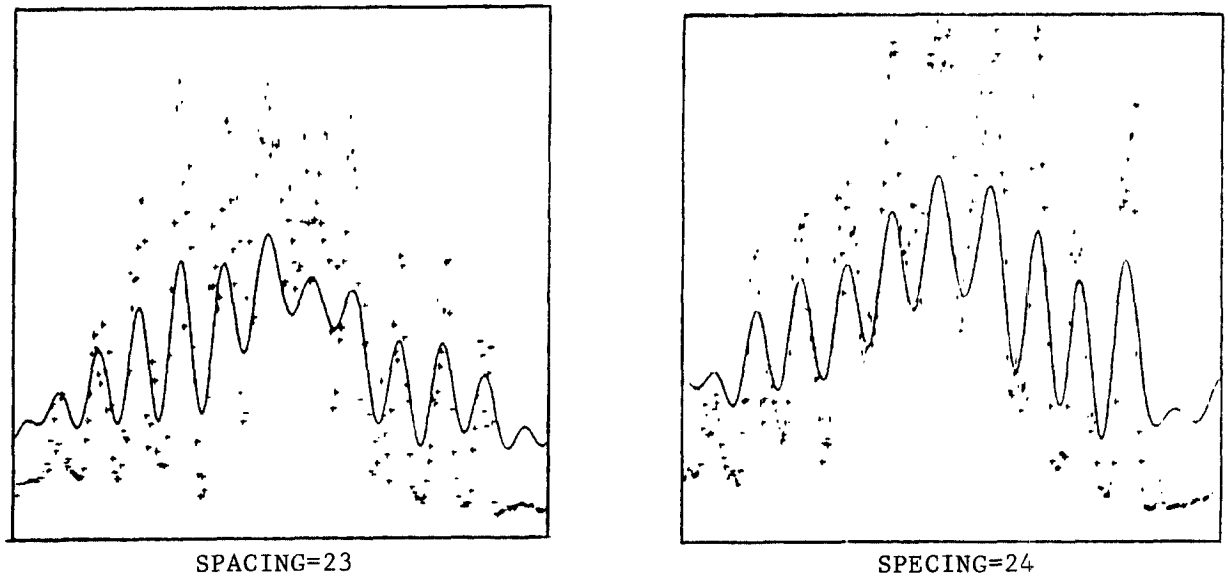

Fig. 3 Plot of fringe pattern intensity

real value for the fringe spacing is obtained.

3. DESCRIPTION OF EXPERIMENTAL PROGRAM

3.1 Specimen Preparation

The C-specimen is included in the ASTM E399, Standard Test Methods for plane strain fracture toughness mainly because of the half-cylindrical shape. Whereas the ASTM standard uses thick specimens, $B=0.5\ W$(Fig. 4) to obtain plane-strain conditions, specimens with $B=0.125W$ was used in these experiments. However, the SIF equations presented in ASTM E399 compensate for these thickness differences. The thinner specimen made it easer to start and control the growth of the crack because a thinner less compliant specimen allows for small controlled changes in the applied load.

The specimens were made out of 1/8 inch thick plexiglass(PMMA) sheets. To make the preparation easier a circular steel template was designed. A ring was roughly cut out of the plexiglass sheet by bandsaw 0.1~0.15 inches bigger than the intended dimension and then superimposed on the template for drilling of the pin-holes. Double adhesive tape was used to keep the specimen "steady" on the template while removing the last 0.1~0.15 inches of excess material by a high speed rotor. The purpose of using a high speed rotor was to get a nice smooth edge without any residual stresses. Finally the ring was cut in half by a bandsaw. The crack was initiated by cutting a chevron-shaped groove with a jeweler saw and then tapping a razor blade in the middle of the chevron. While tapping the specimen was preloaded with approximately 30 lbs. Increasing of the load to about 130 lbs made the crack grow and a constant rate of growth was obtained by decreasing the load continuously.

3.2 The Double Exposure Speckle Photographs

Figure 5 illustrates the set-up for taking the double exposure photographs. An Arogn laser(green) with wavelength= 514.5μm was used mounted with a diverging so called spatial filter giving a circular beam big enough to illuminate the whole specimen. The specimen was painted white in order to get a more distinct speckle-plattern without interference with reflected light from the back surface. To absorb the elasticity and slack in the loading frame, the specimen was preloaded(20 lbs) while taking the first exposure (exposure time 10 seconds). The load was then increased(40 lbs) and the second exposure taken(10 seconds). It should be mentioned that focusing before the exposuree is of great importance in order to obtain a distinct picture of the crack-tip. The specified procedure was used to develop the AGFA-GEVEART 10E75 photographic plates and the resulting specklegram was analysed.

3.3 Rigid Body Motion Effects on Point-by-Point Method

The measured data-values using the point by-point method are total displacements including rigid body motion effects. In addition, it is not possible to determine the direction directly. It is therefore necessary to deduce the deformation directly. It is therefore necessary to deduce the deformation direction due to loading and the direction due to Rigid Body Motion(RBM). In this case both a translational and rotational RBM were considered. From observations of the specimen made during loading it was actually possible to see the

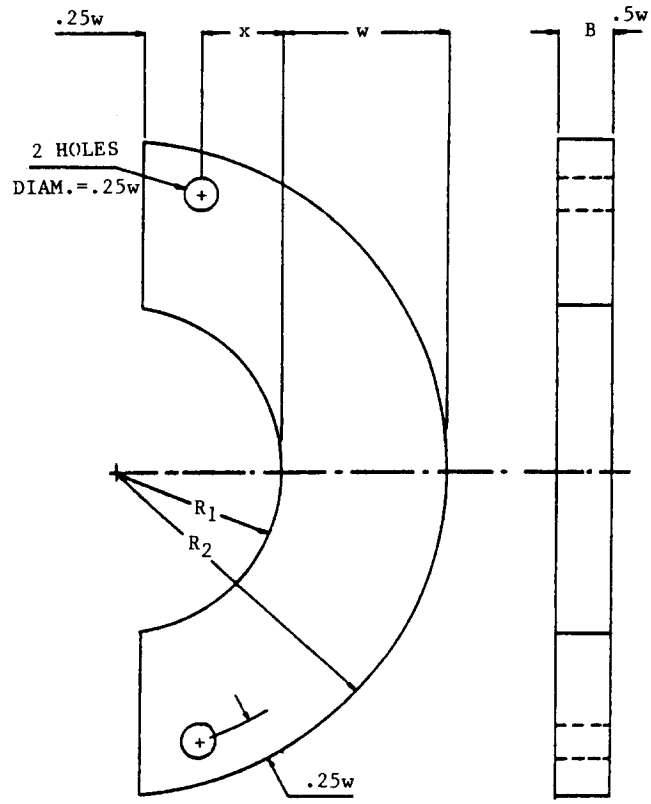

Fig. 4 The standard C-specimen

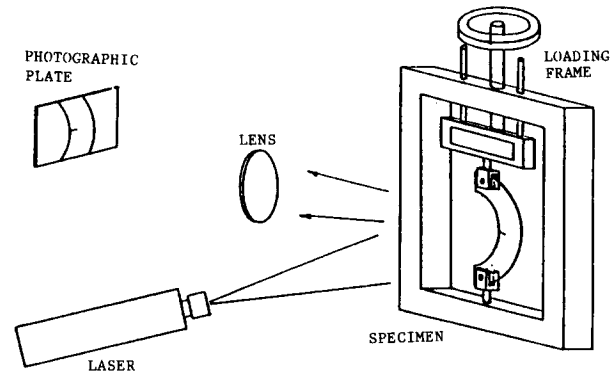

Fig. 5 Setup for double exposure photography

direction of rotation. This was further confirmed y analysis of data taken around the crack. The rotation was caused by an unstable upper part of the loading frame. The bottom attachment was considered fixed and the rotation was therefore around the bottom pin-hole. A great deal of the translational motion in the cracked region was due to the "stretch" of the specimen which when loaded, made the cracked midsection move towards the line of loading. The angle of rotation can be determined by measuring the slope of the v-displacement curve for data taken at $\theta=0$. This cure only appear due to rigid body motion. The v-displacement should be equal to zero along $\theta=0$, for a symmetrical load condition. The curve is shown in Fig. 6. A value of .025 DEG was obtained for the rigid body rotation. To calculate the rotational displacement at any point we define a coordinate

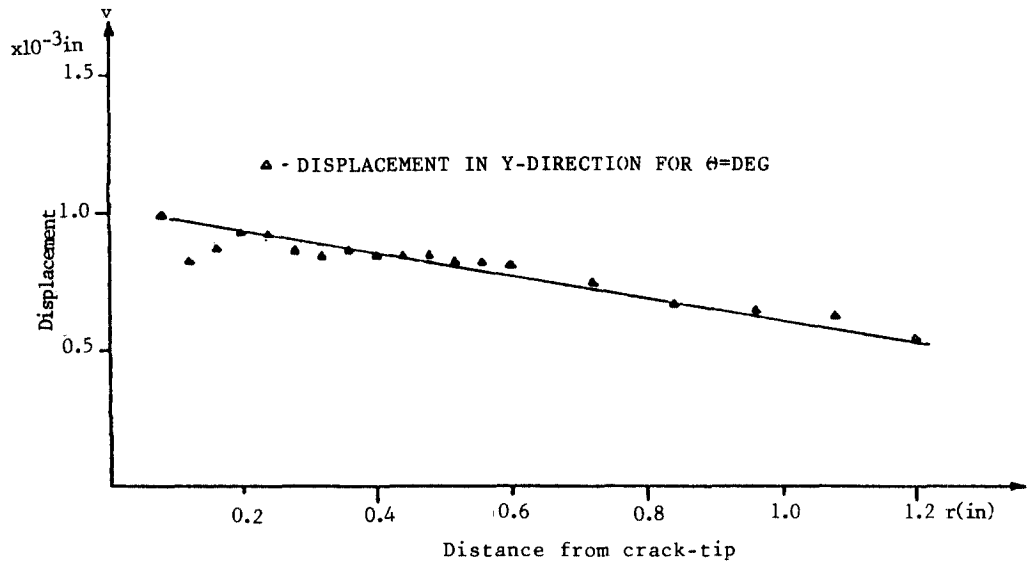

Fig. 6 V-Displacement for data taken at $\theta=0$ DEG

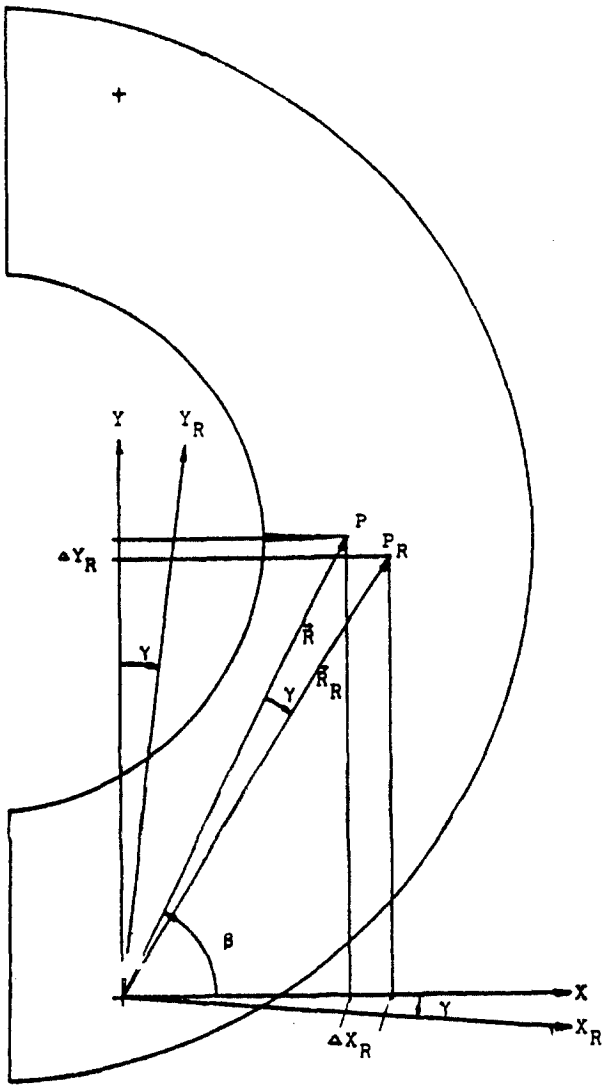

Fig. 7 Definition of rotatonal rigid body motion

system at the point of rotation as shown in Fig. 7 From geometry we obtain the following equations:

$$u_R = R[\cos(\beta-\gamma)-\cos\beta]$$
$$v_R = R[\sin\beta-\sin(\beta-\gamma)] \tag{3}$$

where γ is the angle of rotation. It is now possible to determine the RBM due to rotation at any point defined by R and γ.

The translational of RBM can be determined by considering the fact that the displacement at the crack-tip is equal to zero. It can very be written:

$$u_T = u_M - u_R$$
$$v_T = v_M - v_R \tag{4}$$

where index M stands for measured values. Because of dimpling effects at the crack-tip it was not possible to measure any displacement closer than tehrefore obtained by extrapolating the displacement curves.

The resultant displacement field was compared with the one obtained by the Westergaard solution(1939). The K_I-value used in the Westergaard solution was determined from a wide range K-expression obtained for the C-specimen by Underwood(1980). If the loads at which the specklegram was obtained were P_1 and P_2 then K_I for a certain cracklength will be given by:

$$K_I = K_I(P_2) - K_I(P_1) \tag{5}$$

3.4 Digital Image Processing

This method makes it possible to simplify the very tedious speckle photography method and the time consuming point-by-point data analysis. Instead of recording the reflected speckle pattern from the surface of the specimen on a photographic plate, it is recorded by digitizing a video of the laser illuminated surface. The digitizing process is the same as illustrated in Fig. 2 The two speckle patterns, before and after deformation, are digitized and stored in the computer as

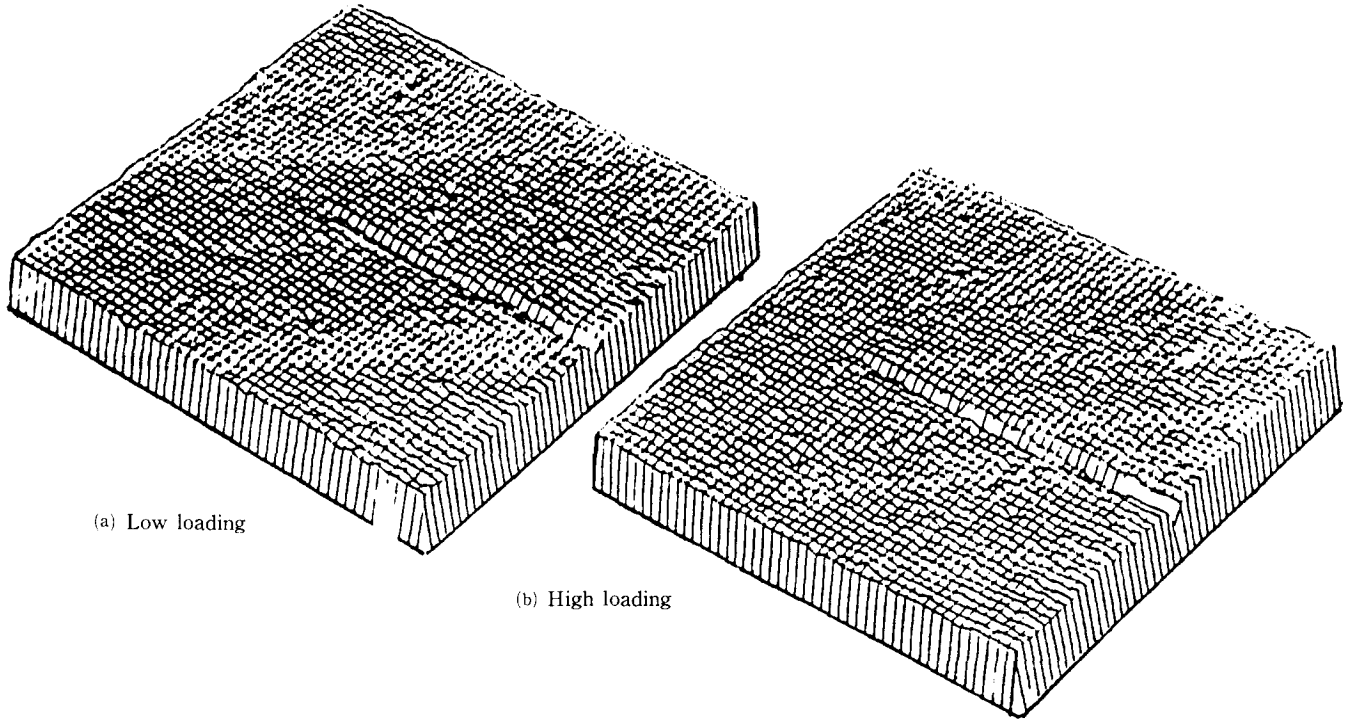

Fig. 8 Digitized image of srface with crack

two arrays of integers. Each integer is related to the light intensity of a point in the speckle pattern. The total size of the array is 240×256. Assigning the array originated in the underformed surface as the reference, it is possible to take a test array(10×10) originated in the deformed surface and correlated it with the reference. Once the test array "finds" the corresponding array in the reference then the displacements can be calculated. The correlation and calculation is done by means of a fortran program.

The advantage of this method is that the rigid body motion can be eliminated by obtaining the displacements with respect to the crack-tip since the crack-tip can be assigned the same pixel location in each array and the correlation carried out after this initial assignment. The speckle patterns of the reference surface and deformed surface in the region of the crack-tip has been digitized. The resulting images are plotted in Fig. 8a and Fig. 8b. The distinct appearance of the crack is very promising with respect to the future use of the correlation program.

4. RESULTS AND DISCUSSION

The dsplacement field obtaind for specimen is plotted in Fig. 9 and Fig. 10 for $\theta=90$ and $\theta=0$ DEG respectively. For comparisn is plotted the displacement field obtained by the Westergaard solution for plane stress(the experimental displacement field is obtained on the stress free surface). Apparently there is only agreement at the region close to the crack-tip. The Westergaard solution that has been used in the comparisn is a solution which neglects higher-order terms in r and is obtained for plane stress or plane strain mode I cases Westergaard (1939). The solution is therefore valid for small values of r only since the influence of the higher order terms increases as the distance from the crack-tip increases. As long as the stress field is prportional to $(r)^{-1/2}$ then it is defined as singular. This singularity only exist in the region close to the crack-tip. For normal tensile specimens where the stress distributon is fairly uniform the singularity can be considered to exist at a greater distance from the crack-tip but for the case of the C-specimen where the stress field changes from tension to compression when approaching the far edge. The remote deformation field must therefore be considered non-local for r greater than $0.1 \sim 0.12$ inches as is shown in the data presented in Fig. 9 and Fig. 10. Also it should be mentioned that the rigid body moton, although compensated for,

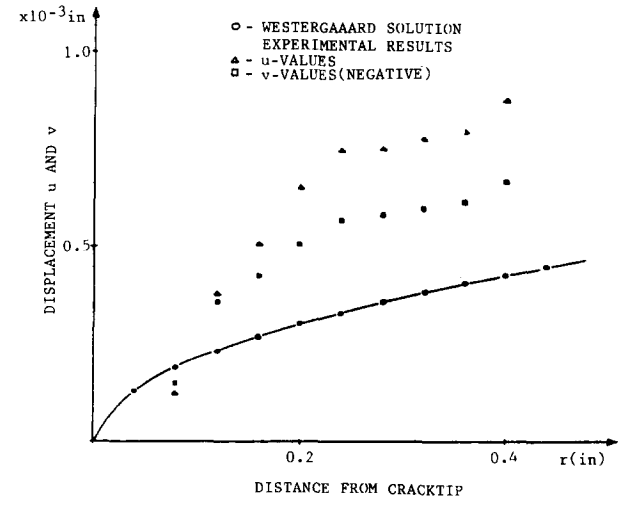

Fig. 9 Displacement graphs for $\theta=90$ DEG

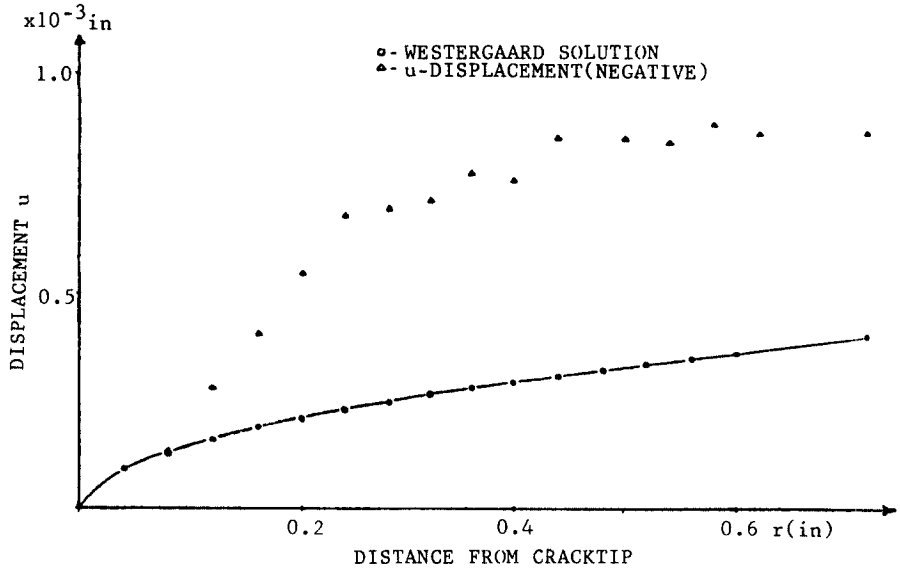

Fig. 10 Displacement graphs for $\theta=0$ DEC

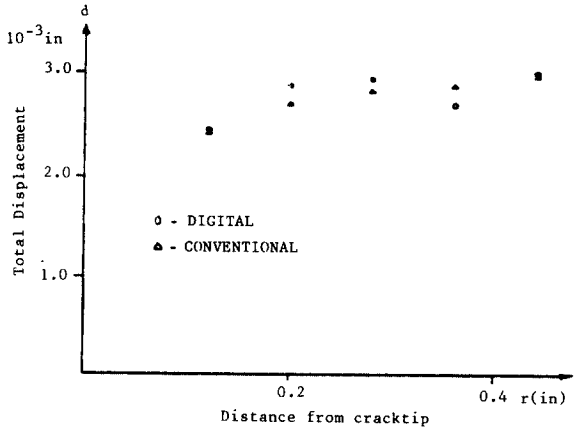

Fig. 11 Total displacements obtained by conventional data analysis and dgital analysis

was 2~3 times larger than the dsplacements associated with the singular field which indicates that the experimental equipment, basically the loading frame allows fo unwanted rigid body motion. The fact that the specimen"stretches" and is very compliant causes the midsection to move in the negative x-diection. The resultant displacements are difficult to account for except in the near crack-tip region.

The application of Digital Fringe Analysis was not extended to all data-points because of the limitatons explained before. Five photographs of diffraction halos obtained for points along the line $\theta=0$ degree were digitized and the results compared with those obtained by the conventional analysis. Since the fringe angle could not be calculated by the digital procedure, the comparisons only carried out for total displacements as shown in the graphs in Fig. 11. The maximum difference between corresponding values was 8%.

5. CONCLUSIONS

Although it was possible to obtain a displacement field by the use of the conventional double exposure speckle photography, results agree with Westergaard soluton only at the region close to the crack-tip. An analytical procedure was developed to account for rigid body translations and rotations. In the near crack-tip region, this procedure was able to accurately account for these rigid body displacements.

The application of computerized correlation of speckle patterns should account for rigid body motion problems and since the accuracy depends only on the digitizing system and the development of the correlation program, this metod will certainly become very useful for future work in Fracture Mechanics.

REFERENCIS

Ennos, A.E., 1968, "Measurement of In-Plate Surface Strain by Hologram Interferometry," Journal of Scientific Instruments, (Journal of Physics E), Vol.1, No.7, pp. 731~734.

Evans, W.T. and Luxmoore, A., 1974, "Measurement of In-plane Displacements Around Crack-Tips by a Laser Speckle Method," Engr. Fracture Mechanics, Vol.6, pp. 735~743.

Kapp, j., Newman, JH. C. and Underwood, j.H., 1980, "A Wide Range K-Expression for the C-Shaped Specimen," Technical Report ARLCB-TR-80009, U.S. Army Armament Research and Development Command, March.

Leendertz, J.A., 1970 "Interferometric Displacement Measurement on Scattering Surfaces Utilizing Speckle Effect," Journal of Scientific Instruments, (Journal of Physics E.) vol. 3, No.3.

Ranson, W.F., Fraley, J.E. and Hamed, M.A., 1981, "Computer Aided Data Analysis in Laser Speckle Metrology," Progress Report.

Stetson, K.A., 1970, "New Design for Laser Image-Speckle Interferometry," Optics and Laser Tech., 2, pp. 179~181.

Westergaard, H.M., 1939, "Bearing Pressures and Cracks," Transactions, Am. Soc. Mech. Engrs., Journal of Applied Mechanics.